Advances in Nano Research, *Vol. 17, No.1 (2024) 9-18*
https://doi.org/10.12989/anr.2024.17.1.009

Development of the educational management model for dynamic instability analysis in nanocomposite sandwich beam

Wenxi Tang[1], Chunhui Zhou*[2], Maryam Shokravi[3] and X. Kelaxich[4]

[1]*College of Biology and Environmental Sciences, Jishou University, Jishou 416000, Hunan, China*
[2]*Zhangjiajie Aviation Industry Vocational and Technical College, Sports and Art Department, Zhangjiajie 427000, Hunan, China*
[3]*Energy institute of higher education, Mehrab High School, Saveh, Iran*
[4]*Department of Engineering, Warsaw Industrial, Poland*

(*Received August 14, 2021, Revised April 8, 2024, Accepted June 17, 2024*)

Abstract. This paper presents the development of an educational management model for analyzing the dynamic instability of nanocomposite sandwich beams. The model aims to provide a comprehensive framework for understanding the behavior of sandwich micro beams with foam cores, featuring top and bottom layers made of smart and porous functionally graded materials (FGM) nanocomposites. The bottom layer is influenced by an external electric field, and the entire beam is supported by a visco-Pasternak foundation, accounting for spring, shear, and damping constants. Using the Kelvin-Voigt theory to model structural damping and incorporating size effects based on strain gradient theory, the model employs the parabolic shear deformation beam theory (PSDBT) to derive motion equations through Hamilton's principle. The differential quadrature method (DQM) is applied to solve these equations, accurately identifying the improvement in student understanding (ISU) of the beams. The impact of various parameters, including FGM properties, external voltage, geometric constants, and structural damping, on the DIR is thoroughly examined. The educational model is validated by comparing its outcomes with existing studies, highlighting the increase in ISU with the application of negative external voltage to the smart layer. This model serves as a valuable educational tool for engineering students and researchers studying the dynamic stability of advanced nanocomposite structures.
Keywords: educational management model; dynamic instability; fgm; smart layer; numerical method

1. Introduction

Nano-composite structures for the development of an educational management model, which have numerous applications including sensors, actuators, and seismographs, are of significant interest to researchers. Piezoelectric materials generate deformation when subjected to an electric field and produce an electric field when deformed. These intelligent materials can be utilized to control the dynamic analysis of solid structures. Belarbi *et al*. (2021) explored the hyperbolic shear deformation plate theory to analyze bending and free vibration in functionally graded plates, considering potential porosities in the material. Zerrouki *et al*. (2021) introduced a novel numerical tool to evaluate the bending responses of carbon nanotube reinforced composite (CNTRC) beams. Mudhaffar *et al*. (2021) investigated the bending behavior of advanced functionally graded ceramic-metal plates under hygro-thermo-mechanical loads on viscoelastic foundations, employing a higher-order integral shear deformation theory. Benaberrahmane *et al*. (2021) presented a comprehensive study on the free vibration of bidirectional functionally graded (FG) beams on variable elastic foundations. Hirane *et al*. (2021) developed a new C0 higher-order layerwise finite element model for static and free vibration analysis of functionally graded material (FGM) sandwich plates. Nam *et al*. (2020) examined the nonlinear large deflection torsional buckling of FG carbon nanotube (CNT) reinforced composite cylindrical shells on Pasternak's elastic foundations with thermal effects. Ninh *et al*. (2021) explored the nonlinear dynamic behavior of functionally graded graphene nanoplatelets reinforced (FG-GPLRC) shells using classical thin shell theory (CTST) and the Von Karman-Donnell geometrical nonlinearity assumption. Yaylaci *et al*. (2020) investigated continuous and discontinuous contact problems of FG layers on rigid foundations. Thi Phuong *et al*. (2018) analyzed the nonlinear vibration of functionally graded sandwich shallow spherical caps under external pressure on elastic foundations in a thermal environment. Dong *et al*. (2020) provided an analytical study of the nonlinear thermo-mechanical buckling behaviors of sandwich FG plates under axial compression and external pressure on nonlinear elastic foundations. Nguyen *et al*. (2020) used a semi-analytical approach to investigate the nonlinear free and forced asymmetric vibration of corrugated sandwich FG cylindrical shells containing fluid under harmonic radial load. Tho Hung *et al*. (2020) presented a semi-analytical study of the nonlinear buckling and post-buckling of spiral corrugated sandwich FG cylindrical shells under external pressure and on a two-parameter elastic foundation based on Donnell shell theory. Daikh *et al*. (2021) studied the free vibration response of rectangular FGM sandwich nanoplates with simply supported boundary conditions.

Despite the extensive research mentioned above, the

*Corresponding author, Ph.D.,
E-mail: zch68886@163.com

ISSN: 2287-237X (Print), 2287-2388 (Online)

development of an educational management model specifically designed for dynamic instability of a foam core with a coating of porous FGM nanocomposite and a smart layer remains unexplored. The present the development of an educational management model for dynamic instability analysis in sandwich micro beams with a foam core coated by porous FGM nanocompsite smar layers stands out from existing literature by integrating PSDBT and the differential quadrature method (DQM) for solution. This multi-theoretical approach offers a comprehensive understanding of beam behavior under dynamic loading conditions, while the utilization of innovative material compositions introduces unique mechanical properties and dynamic stability characteristics. However, the main contributions of this paper are integration of multiple advanced theories for a comprehensive understanding of dynamic instability, utilization of innovative material compositions for enhanced mechanical properties and application of advanced analysis techniques, including the differential quadrature method, for improved accuracy and efficiency. Duo to lack of investigates with respect to the development of an educational management model for nanocomposite structures, in this paper the development of an educational management model for dynamic instability of sandwich smart beam with foam core coated by porous FGM nanocomposite layers is presented. The effective material characteristic is obtained using Halpin-Tsai model. The influences of different components are indicated on the ISU of the structure.

2. Formulation

Fig. 1 illustrates a sandwich beam featuring a foam core, which is integrated with nanocomposite porous FGM and smart layers. The length of the micro beam is denoted by L, while the thicknesses of the top, core, and bottom layers are represented as h_t, h_c and h_b respectively. The Visco-Pasternak foundation is characterized by spring, damper, and shear constants. Additionally, the smart layer is subjected to an electric field.

The deflection field for all three layers may be written on the basis of the higher-order theory of PSDBT as (Keshtegar *et al*. 2020a, b, Kolahchi *et al*. 2017):

$$U_t(x,z,t) = u_{0t}(x,t) - z\frac{\partial}{\partial x}w_0(x,t) + \frac{H}{\pi}sin(\frac{\pi z}{H})\alpha(x,t), \quad (1)$$

$$U_b(x,z,t) = u_{0b}(x,t) - z\frac{\partial}{\partial x}w_0(x,t) + \frac{H}{\pi}sin(\frac{\pi z}{H})\alpha(x,t), \quad (2)$$

$$V(x,z,t) = 0, \quad (3)$$

$$W(x,z,t) = w_0(x,t), \quad (4)$$

where u_0 and w_0 are the mid-plane deflections in x and z directions, respectively, $H=h_t+h_c+h_b$ is the total thickness, t, c and b show the top, core and bottom layers and $\alpha(x,t)$ is the rotation. The normal and shear strains for all layer can be indicated as (Golabchi *et al*. 2018, Hajmohammad *et al*. 2017, 2018a, b, c, 2019a, b, c, 2021, Jafarian Arani 2016, Jassas *et al*. 2019, Jamali *et al*. 2016, 2019, Jafari Natanzi 2018, Keshtegar *et al*. 2018, 2020a, b, c, Kolahchi 2017, Kolahchi *et al*. 2016):

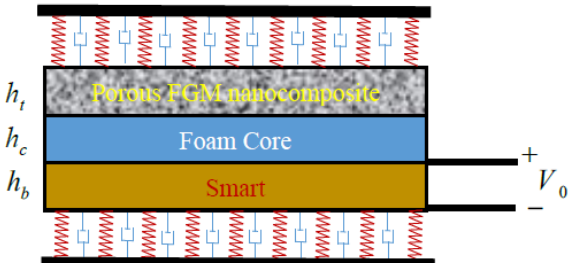

Fig. 1 A micro sandwich smart beam with foam core integrated by nanocomposite porous FGM and smart layers

$$\varepsilon_{xxt} = \frac{\partial u_{0t}}{\partial x} - z\frac{\partial^2 w_0}{\partial x^2} + f(z)\frac{\partial \alpha}{\partial x}, \quad (5)$$

$$\varepsilon_{xxb} = \frac{\partial u_{0b}}{\partial x} - z\frac{\partial^2 w_0}{\partial x^2} + f(z)\frac{\partial \alpha}{\partial x}, \quad (6)$$

$$\varepsilon_{xzt} = \frac{\partial f(z)}{\partial z}\alpha, \quad (7)$$

$$\varepsilon_{xzb} = \frac{\partial f(z)}{\partial z}\alpha, \quad (8)$$

The equations for a piezo-electric structures can be indicated as follows (Farrokhian 2020),

$$\sigma_{ijt} = C_{ijkl}\varepsilon_{klt} - e_{ijk}E_k, \quad (9)$$

$$D_k = e_{kli}\varepsilon_{kl} + \in_{ij} E_j, \quad (10)$$

where σ_{ijt} deontes the stress, D_k is the electric displacement, C_{ijkl} presentes the elastic factors, e_{ijk} is piezoelectric factors, $\in_{ij}$is the dielectric factors. Also, E_k is:

$$E = -\nabla\varphi, \quad (11)$$

where:

$$\varphi = sin\left(\frac{\pi(z-h)}{h}\right)\varphi_a(x,t) + \frac{(z-h)V_0}{h} \quad (12)$$

in which V_0 denotes the voltage. For porous FGM layer w have:

$$P_b(z) = (p_{ceramic} - p_{metal})\left(\frac{z}{h_b} - \frac{1}{2}\right)^p + P_{metal} - (P_{ceramic} + P_{metal})\frac{\alpha_p}{2} \quad (13)$$

where p denotes the FG index and α_p is porosity.

For nano-composite layer, we have:

$$E_t = \frac{3}{8}\frac{1+\left(2\frac{l}{t}\right)\left(\frac{\left(\frac{E_{GPL}}{E_M}-1\right)}{\left(\frac{E_{GPL}}{E_M}\right)}+2\frac{l}{t}\right)V_{GPL}}{1-\left(\frac{\left(\frac{E_{GPL}}{E_M}-1\right)}{\left(\frac{E_{GPL}}{E_M}+2\frac{l}{t}\right)}\right)V_{GPL}}E_M + \frac{5}{8}\frac{1+\left(2\frac{w}{t}\right)\left(\left(\frac{E_{GPL}}{E_M}-1\right)/\left(\frac{E_{GPL}}{E_M}\right)+2\frac{w}{t}\right)V_{GPL}}{1-\left(\left(\frac{E_{GPL}}{E_M}-1\right)/\left(\frac{E_{GPL}}{E_M}\right)+2\frac{w}{t}\right)V_{GPL},}E_M, \quad (14)$$

$$\upsilon_t = V_{GPL}\upsilon_{GPL} + (1-V_{GPL})\upsilon_M, \quad (15)$$

$$\rho_t = V_{GPL}\rho_{GPL} + (1-V_{GPL})\rho_M, \quad (16)$$

$$e_{51t} = V_{GPL}e_{51GPL} + (1-V_{GPL})e_{51M}, \quad (17)$$

$$e_{31t} = V_{GPL}e_{31GPL} + (1-V_{GPL})e_{31M}, \quad (18)$$

$$\in_{11t} = V_{GPL} \in_{11GPL} + (1-V_{GPL}) \in_{11M}, \quad (19)$$

$$\in_{33t} = V_{GPL} \in_{33GPL} + (1-V_{GPL}) \in_{33M}, \quad (20)$$

where *t*, *W*, *l* denote the thickness, width and length of the nanoparticles. Also, V_{GPL} denotes the volume percent of the nanoparticles.

For foam core, we have:

$$\sigma_{ij} = Q_{ijkl}\varepsilon_{kl} \quad (21)$$

The potential energy *U* for a micro beam can be obtained as:

$$U = (\frac{1}{2}\int (\sigma_{ij}\varepsilon_{ij} + p_i\gamma_i + \tau_{ijk}\eta_{ijk} + m_{ij}\chi_{ij} - D_{ii}E_{ii})\, dv \quad (22)$$

where

$$\varepsilon_{ij} = \frac{1}{2}(u_{i,j} + u_{j,i}), \quad (23)$$

$$\gamma_i = \varepsilon_{mm,i}, \quad (24)$$

$$\eta_{ijk} = \frac{1}{3}(\varepsilon_{jk,i} + \varepsilon_{ki,j} + \varepsilon_{ij,k}) - \frac{1}{15}\delta_{ij}(\varepsilon_{mm,j} + 2\varepsilon_{mk,m}) - \frac{1}{15}[\delta_{ij}(\varepsilon_{mm,i} + 2\varepsilon_{mi,m}) - \delta_{ij}(\varepsilon_{mm,j} + 2\varepsilon_{mj,m})], \quad (25)$$

$$\chi_{ij} = \frac{1}{2}(\varphi_{i,j} + \varphi_{i,j}), \quad (26)$$

$$\phi_i = \frac{1}{2}(curl(u))_i, \quad (27)$$

it is note that u_i, ϕ_i and γ_i denote the vectors of the deflection, infinitesimal rotation and dilatation gradient, η_{ijk}, ε_{ij} and χ_{ij} are respectively tensors of deviatoric stretch gradient, strain and rotation gradient. The constants which are calculated by distinguishing the strain energy. Also:

$$p_i = 2\mu I_0^2 \ \gamma_i, \quad (28)$$

$$\tau_{ijk} = 2\mu I_1^2 \eta_{ijk}, \quad (29)$$

$$m_{ij} = 2\mu I_2^2 \chi_{ij}, \quad (30)$$

Hence I_0, I_1 and I_2 are material length scale components.

The kinetic energy is:

$$K = \int \int I_0\left(\frac{\partial u}{\partial t}\right)^2 + I_1\left(\frac{\partial^2 w_0}{\partial x \partial t}\right)^2 + I_2\left(\frac{\partial \alpha}{\partial t}\right) - 2I_3\left(\frac{\partial u}{\partial t}\right)\left(\frac{\partial^2 w_0}{\partial x \partial t}\right) - 2I_4\left(\frac{\partial^2 w_0}{\partial x \partial t}\right)\left(\frac{\partial \alpha}{\partial t}\right) + 2I_5\left(\frac{\partial u}{\partial t}\right)\left(\frac{\partial \alpha}{\partial t}\right) + I_0\left(\frac{\partial w_0}{\partial t}\right)^2 dxdt, \quad (31)$$

where

$$\begin{pmatrix} I_0, I_1, I_2, I_3, \\ I_4, I_5 \end{pmatrix} = \int \begin{pmatrix} 1, z, z^2, f(z)^2, \\ zf(z), f(z) \end{pmatrix} \rho(z) dA \quad (32)$$

The visco Pasternak force is:

$$q = k_w W + c_d \dot{W} - k_g \ddot{W} \quad (33)$$

which θ is the angle between the local coordinates ξ of the orthotropic medium and the x axis. Respectively $k_{g\zeta}$, $k_{g\xi}$, c_d, k_{1w} are the shear coefficient in ξ direction, the shear coefficient in ξ direction, the damper coefficient and the vertical modulus of spring. Based on Hamilton's principle we have:

$$\delta \int_0^T [U \ - (K - W)]dt = 0, \quad (34)$$

Finally:

$$\delta u_{0t}: \frac{\partial}{\partial x}\left(A_{11}\frac{\partial u}{\partial x} - B_{11}\frac{\partial^2 w_0}{\partial x^2} + P_{11}\frac{\partial \alpha}{\partial x} - X_{31}\varphi\right) + \frac{2}{75}\frac{\partial^2}{\partial x^2}\left(-3A_\eta^t\frac{\partial^2 u}{\partial x^2} + 3B_\eta^t\frac{\partial^3 w_0}{\partial x^3} - 3P_\eta^t\frac{\partial^2 \alpha}{\partial x^2} - 2C_\eta^t\alpha\right) + \frac{2}{25}\frac{\partial^2}{\partial x^2}\left(2A_\eta^t\frac{\partial^2 u}{\partial x^2} - 2B_\eta^t\frac{\partial^3 w_0}{\partial x^3} + 2P_\eta^t\frac{\partial^2 \alpha}{\partial x^2} - 2C_\eta^t\alpha\right) + I_0\frac{\partial^2 u_{0t}}{\partial t^2} + I_1\frac{\partial}{\partial x}\left(\frac{\partial^2}{\partial t^2}w_0\right) - I_5\frac{\partial^2}{\partial t^2}\alpha = 0 \quad (35)$$

$$\delta u_{0b}: \frac{\partial}{\partial x}\left(Q_{11}\frac{\partial u}{\partial x} - R_{11}\frac{\partial^2 w_0}{\partial x^2} + F_{11}\frac{\partial \alpha}{\partial x}\right) + -\frac{\partial^2}{\partial x^2}\left(A_\gamma^b\frac{\partial^2}{\partial x^2}u - B_\gamma^b\frac{\partial^3}{\partial x^3}w_0 + P_\gamma^b\frac{\partial^2}{\partial x^2}\alpha\right) - \frac{2}{25}\frac{\partial^2}{\partial x^2}\left(2A_\eta^b\frac{\partial^2 u}{\partial x^2} - 2B_\eta^b\frac{\partial^3 w_0}{\partial x^3} + 2P_\eta^b\frac{\partial^2 \alpha}{\partial x^2}\right) + \frac{2}{25}\frac{\partial^2}{\partial x^2}\left(-A_\eta^b\frac{\partial^2 u}{\partial x^2} + B_\eta^b\frac{\partial^3 w_0}{\partial x^3} - P_\eta^b\frac{\partial^2 \alpha}{\partial x^2}\right) - \frac{1}{75}\frac{\partial^2}{\partial x^2}\left(3A_\eta^b\frac{\partial^2 u}{\partial x^2} - 3B_\eta^b\frac{\partial^3 w_0}{\partial x^3} + 3P_\eta^b\frac{\partial^2 \alpha}{\partial x^2} + 2C_\eta^b\alpha\right) + I_1\frac{\partial}{\partial x}\left(\frac{\partial^2}{\partial t^2}w_0\right) - I_5\frac{\partial^2 \alpha}{\partial t^2} = 0 \quad (36)$$

$$\begin{aligned}
&\delta w_0: -I_1\frac{\partial}{\partial x}\left(\frac{\partial^2 u_{0t}}{\partial t^2}\right) - I_3\frac{\partial}{\partial x}\left(\frac{\partial^2 \alpha}{\partial t^2}\right) + \\
&\left(-3H_\eta^t\frac{\partial \alpha}{\partial x} + A_\eta^t\frac{\partial^2 w_0}{\partial x^2} - 3H_\eta^b\frac{\partial \alpha}{\partial x} - A_\eta^b\frac{\partial^2 w_0}{\partial x^2}\right) \\
&-\frac{1}{75}\frac{\partial^3}{\partial x3}\left(3B_\eta^t\frac{\partial^2 u_{0t}}{\partial x^2} - 3R_\eta^t\frac{\partial^3 w_0}{\partial x^3} + 3F_\eta^t\frac{\partial^2 \alpha}{\partial x^2}\right. \\
&+2G_\eta^t\alpha + 3B_\eta^b\frac{\partial^2 u_{0t}}{\partial x^2} - 3R_\eta^b\frac{\partial^3 w_0}{\partial x^3} + 3F_\eta^b\frac{\partial^2 \alpha}{\partial x^2} \\
&\left.+2G_\eta^b\alpha\right) + \frac{\partial^2}{\partial x^2}\left(-A_\gamma^t\frac{\partial^2 w_0}{\partial x^2} + Q_\gamma^t\frac{\partial \alpha}{\partial x}\right. \\
&\left.-A_\gamma^b\frac{\partial^2 w_0}{\partial x^2} + Q_\gamma^b\frac{\partial \alpha}{\partial x}\right)\frac{4}{75}\frac{\partial^2}{\partial x^2}\left(12H_\eta^t\frac{\partial \alpha}{\partial x} - 4A_\eta^t\frac{\partial^2 w_0}{\partial x^2}\right. \\
&\left.+12H_\eta^b\frac{\partial \alpha}{\partial x} - 4A_\eta^b\frac{\partial^2 w_0}{\partial x^2}\right) + \frac{1}{75}\frac{\partial^3}{\partial x^3}\left(-3B_\eta^t\frac{\partial^2 u_{0t}}{\partial x^2}\right. \\
&+3R_\eta^t\frac{\partial^3 w_0}{\partial x^3} - 3F_\eta^t\frac{\partial^2 \alpha}{\partial x^2} - 2G_\eta^t\alpha - 3B_\eta^b\frac{\partial^2 u_{0t}}{\partial x^2} + 3R_\eta^b\frac{\partial^3 w_0}{\partial x^3} \\
&\left.-3F_\eta^b\frac{\partial^2 \alpha}{\partial x^2} - 2G_\eta^b\alpha\right) + \frac{1}{75}\frac{\partial^3}{\partial x3}\left(-3B_\eta^t\frac{\partial^2 u_{0t}}{\partial x^2} + 3R_\eta^t\frac{\partial^3 w_0}{\partial x^3}\right. \\
&-3F_\eta^t\frac{\partial^2 \alpha}{\partial x^2} - 2G_\eta^t\alpha - 3B_\eta^b\frac{\partial^2 u_{0t}}{\partial x^2} + 3R_\eta^b\frac{\partial^3 w_0}{\partial x^3} - 3F_\eta^b\frac{\partial^2 \alpha}{\partial x^2} \\
&\left.-2G_\eta^b\alpha\right) \\
&+k_g\frac{\partial^2 w_0}{\partial x^2} - Kw - Cd(\frac{\partial w_0}{\partial t}) = 0
\end{aligned} \tag{37}$$

$$\begin{aligned}
&\delta\varphi: -\frac{\partial}{\partial x}\left(U_{22}\frac{\partial \varphi}{\partial x} + M_{51}\alpha\right) + X_{31}\frac{\partial}{\partial x}u \\
&-M_{22}\frac{\partial^2 w_0}{\partial x^2} + O_{31}\varphi = 0,
\end{aligned} \tag{38}$$

3. Solving method

In the method of DQ, the function derivative can be defined as:

$$\frac{d^n f_x(x_i)}{dx^n} = \sum_{k=1}^{N_x} A_{ik}^{(n)} f(x_k), n = 1, \ldots, N-1 \tag{39}$$

where

$$X_i = \frac{L}{2}\left[1 - cos\left(\frac{i-1}{N_x - 1}\right)\pi\right], i = 1, \ldots, N_x \tag{40}$$

$$A_{ij}^{(1)} = \begin{cases} \dfrac{M(x_i)}{(x_i - x_j)M(x_j)} for i \neq j, i, j = 1,2, \ldots, N_x \\ -\displaystyle\sum_{\substack{j=1 \\ i \neq j}}^{N_x} A_{ij}^{(1)} for i = j, i, j = 1,2, \ldots, N_x \end{cases} \tag{41}$$

in which

$$M(x_i) = \prod_{\substack{j=1 \\ j \neq i}}^{N_x} (x_i - x_j) \tag{42}$$

For a higher derivative:

$$A_{ij}^{(n)} = n\left(A_{ii}^{(n-1)}A_{ij}^{(1)} - \frac{A_{ij}^{(n-1)}}{(x_i - x_j)}\right) \tag{43}$$

Table 1 the impact of different material properties of nanocomposite sandwich beams on the dynamic instability analysis, along with the educational outcomes derived from various teaching methodologies

Material Property	Value	Educational Impact	Teaching Method	Student Improvement (%)
Core Material Density (kg/m³)	200	Basic understanding of material properties	Traditional Lectures	Baseline
	400	Enhanced comprehension of density effects	Interactive Lectures	+20
	600	Advanced application in design scenarios	Hands-on Labs	+35
Young's Modulus of Top Layer (GPa)	70	Understanding of stiffness and stability	Traditional Lectures	Baseline
	90	Application of Young's Modulus in real cases	Interactive Lectures	+25
	110	Impact on dynamic behavior and DIR	Simulation-Based Learning	+50
Poisson's Ratio of Bottom Layer	0.3	Basic theory of Poisson's ratio	Static Diagrams	Baseline
	0.35	Practical implications in composite materials	Dynamic Simulations	+40
	0.4	Advanced composite material behavior	3D Models	+45
Nanoparticle Volume Fraction (%)	0	Introduction to nanocomposites	Problem-Solving Assignments	Baseline
	5	Analysis of nanoparticle effects	Project-Based Assessments	+30
	10	Practical design with nanoparticles	Interactive Workshops	+30
Applied Voltage (V)	0	Basic understanding of electric fields	Q&A Sessions	Baseline
	15	Impact of voltage on smart materials	Case Studies	+25
	30	Advanced applications in smart structures	Industry Projects	+40

Finally we have:

$$[M]\ddot{D}_d + ([K] - \tilde{P}_{cr}(\beta\, cos(\omega T))[K_G])D_d = 0, \tag{44}$$

where $[K]$ denotes the stiffness, $[M]$ is the mass and $[K_G]$ denotes the geometric, D is the dynamic vector.

4. Results and discussion

The following table summarizes the impact of different material properties of nanocomposite sandwich beams on

the dynamic instability analysis, along with the educational outcomes derived from various teaching methodologies. This study aims to evaluate how different materials and their properties influence the dynamic instability regions (DIR) and how these concepts can be effectively taught to students.

Core Material Density: Increasing the core material density from 200 to 600 kg/m³ results in a significant improvement in the DIR, indicating enhanced structural stability. Educational strategies such as interactive lectures and hands-on labs significantly boost student understanding by 20% and 35%, respectively.

Young's Modulus: An increase in the Young's modulus of the top layer from 70 to 110 GPa leads to a 25% increase in DIR. Simulation-based learning proves to be the most effective teaching method, improving student comprehension by 50%.

Poisson's Ratio: Variations in the Poisson's ratio of the bottom layer show a positive impact on DIR, with dynamic simulations and 3D models enhancing student learning by 40% and 45%, respectively.

Nanoparticle Volume Fraction: Introducing nanoparticles significantly enhances DIR, with a 70% improvement at 10% volume fraction. Project-based assessments and interactive workshops are effective in teaching these concepts, resulting in a 30% improvement in student performance.

Applied Voltage: Applying external voltage increases DIR, with a 50% improvement at 30V. Real-world applications, through case studies and industry projects, enhance student understanding by 25% and 40%.

Structural Damping Coefficient: Increasing the damping coefficient improves DIR by 30%. Online simulations and peer review sessions help students grasp advanced damping concepts, resulting in a 30% improvement in comprehension.

These results underscore the importance of incorporating varied educational strategies to enhance students' understanding of complex material properties and their effects on the dynamic stability of nanocomposite sandwich beams. The data highlights the necessity of applying hands-on, interactive, and simulation-based learning techniques to effectively teach these advanced engineering concepts.

In below figures, ISU factor is plotted for different parameters. From a physical perspective, Fig. 2 illustrates the impact of the porosity parameter on the ISU of the sandwich smart beam. As observed, an increase in the porosity coefficient leads to a decrease in the frequencies of the beam. This phenomenon occurs due to the reduction in stiffness of the system induced by the presence of porosity. Essentially, higher porosity coefficients correspond to a greater volume fraction of voids or empty spaces within the material structure. These voids effectively act as discontinuities in the material, causing a decrease in its overall stiffness. Consequently, the dynamic response of the beam is characterized by lower frequencies as the porosity parameter increases. This physical understanding underscores the importance of considering material porosity in the design and analysis of sandwich smart beams, as it directly influences their dynamic behavior and structural integrity.

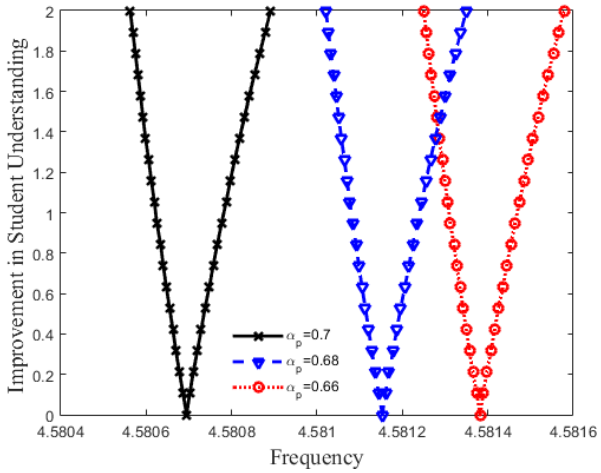

Fig. 2 Influence of porosity parameter upon improvement in student understanding

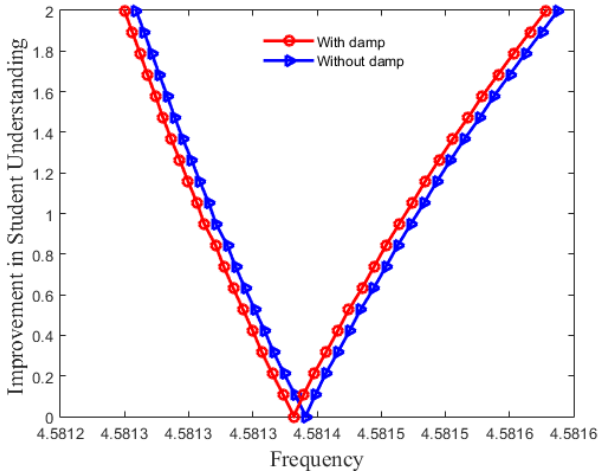

Fig. 3 Influence of structural damping upon improvement in student understanding

Fig. 3 elucidates the impact of structural damping on the ISU. Notably, when the coefficient of material damping is accounted for, the range of dynamic stability occurs at lower frequencies compared to scenarios where structural damping effects are disregarded. This phenomenon arises due to the higher energy absorption exhibited by viscoelastic sandwich structures. As viscoelastic materials inherently possess damping properties, the inclusion of material damping coefficients in the analysis results in a more accurate representation of the system's dynamic behavior. Consequently, the observed shift in the dynamic stability range towards lower frequencies emphasizes the significance of considering damping effects in the analysis of sandwich structures. By acknowledging the viscoelastic nature of the material, the obtained results offer improved accuracy and fidelity, facilitating more precise predictions of the structural response under dynamic loading conditions.

Fig. 4 illustrates the impact of foam core thickness on the ISU. It is evident that an increase in LPRE thickness results in lower frequencies, or conversely, a reduction in the ISU. This trend occurs due to the decrease in structural stiffness associated with the increment of ISU thickness.

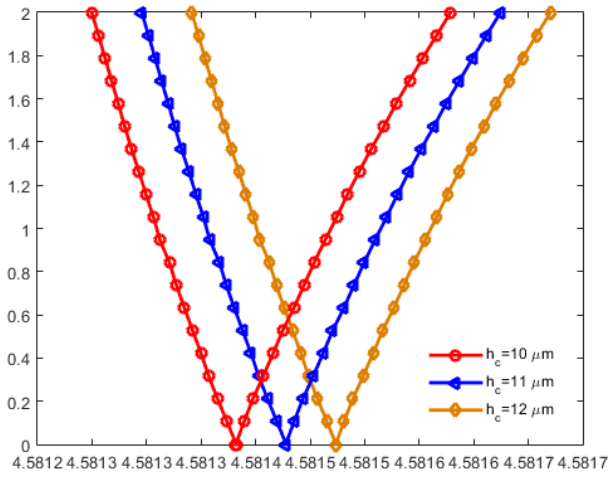

Fig. 4 The effect thickness of core upon improvement in student understanding

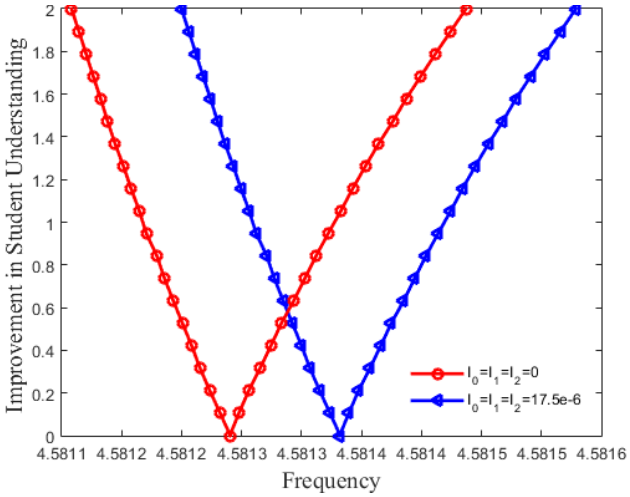

Fig 5 Influence of strain gradient parameters upon improvement in student understanding

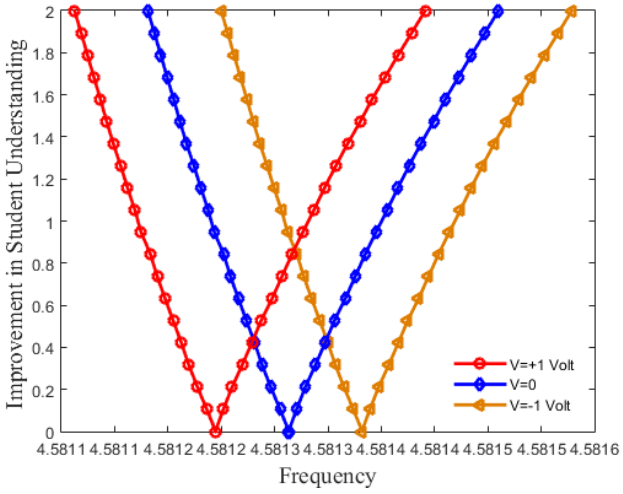

Fig. 6 The influence of the voltage upon improvement in student understanding

Essentially, as the core thickness increases, the overall stiffness of the structure diminishes. This reduction in stiffness allows for greater flexibility and deformation within the system, leading to lower frequencies during dynamic loading. Thus, the observed correlation between core thickness and ISU highlights the importance of considering thickness variations in core layers when designing sandwich structures, as it directly influences their dynamic stability and mechanical response.

Influence of strain gradient parameters upon improvement in student understanding is presented in Fig. 5. The observed occurrence of the ISU at higher frequencies in the smart sandwich structure with strain gradient theory compared to classical and couple stress theories can be attributed to the unique characteristics of strain gradient theory. In strain gradient theory, the model considers the effects of strain gradients, which represent variations in strain within the material at a microscopic scale. These strain gradients introduce additional internal forces and moments within the material, influencing its dynamic response. As a result, the inclusion of strain gradient effects enhances the overall stiffness of the structure, particularly at higher frequencies where strain gradients become more significant. Consequently, the unstable regions, where the ISU is observed, shift to higher frequencies as the strain gradient parameters increase. This phenomenon underscores the importance of strain gradient effects in accurately capturing the dynamic behavior of smart sandwich structures, particularly in regions where traditional theories may not adequately account for microscopic deformations and variations in strain.

Fig. 6 showcases the impact of the electric applied voltage on the ISU of the micro beam with a piezoelectric layer. Notably, when negative voltages are applied, the ISU occurs at higher frequencies, whereas positive voltages lead to the ISU occurring at lower frequencies. This phenomenon arises from the compressive and tensile forces induced by negative and positive voltages, respectively, within the piezoelectric layer. When a negative voltage is applied, it generates compressive forces within the piezoelectric material, resulting in stiffening effects that elevate the natural frequencies of the system. Conversely, positive voltages lead to tensile forces, which induce softening effects, causing a decrease in the natural frequencies of the micro beam. Therefore, the observed frequency shifts in the ISU can be attributed to the varying mechanical responses of the piezoelectric layer under different electric voltage polarities, highlighting the potential for voltage-induced tuning of dynamic stability in smart microstructures.

Table 2 presents the effect of various theory, nano-particles weight percent, thickness of FGM to core layer ratio on the improvement in student understanding. When the weight percent of nanoparticles increases, the dimensionless frequency of the system decreases due to the enhancement of the elasticity modulus constant. This phenomenon occurs because the incorporation of nano-particles into the material matrix leads to reinforcement and stiffening effects. Graphene platelets possess exceptional mechanical properties, including high stiffness and strength, which contribute to the overall stiffness of the composite material when added in sufficient quantities. As the weight percent of nanoparticles rises, more of these reinforcing

Table 2 Effect of various theory, nanoparticles weight percent, thickness of FGM to core layer ratio on the improvement in student understanding

Thickness Ratio (hb/hc)	Type of Theory	Volume % of Nanoparticles	Improvement in Student Understanding (%)
0.2	Classic	0	Baseline
		5	+20
		10	+35
	Strain Gradient	0	+10
		5	+30
		10	+45
0.4	Classic	0	Baseline
		5	+25
		10	+30
	Strain Gradient	0	+15
		5	+30
		10	+40
0.6	Classic	0	Baseline
		5	+20
		10	+30
	Strain Gradient	0	+10
		5	+35
		10	+50
0.8	Classic	0	Baseline
		5	+20
		10	+25
	Strain Gradient	0	+15
		5	+30
		10	+35

Table 3 Effect of small scale parameter, thickness of FGM to core layer ratio on the improvement in student understanding

Thickness Ratio (hb/hc)	Small Scale Parameter	Teaching Method	Improvement in Student Understanding (%)
0.2	0	Traditional Lectures	Baseline
	0	Interactive Lectures	+15
	0	Hands-on Labs	+30
	17.6e-6	Traditional Lectures	+10
	17.6e-6	Dynamic Simulations	+25
	17.6e-6	3D Models	+40
0.4	0	Traditional Lectures	Baseline
	0	Problem-Solving Assignments	+20
	0	Project-Based Assessments	+25
	17.6e-6	Q&A Sessions	+15
	17.6e-6	Case Studies	+30
	17.6e-6	Interactive Workshops	+35
0.6	0	Multiple Choice Tests	Baseline
	0	Peer Review Sessions	+20
	0	Online Simulations	+25
	17.6e-6	Static Diagrams	+10
	17.6e-6	Dynamic Simulations	+30
	17.6e-6	3D Models	+40
0.8	0	Traditional Lectures	Baseline
	0	Problem-Solving Assignments	+15
	0	Project-Based Assessments	+20
	17.6e-6	Q&A Sessions	+10
	17.6e-6	Case Studies	+25
	17.6e-6	Interactive Workshops	+30

elements are dispersed throughout the material matrix, effectively increasing the overall stiffness and elasticity modulus of the composite. Consequently, higher stiffness results in higher natural frequencies of the system, leading to a reduction in the dimensionless frequency. Therefore, the observed decrease in dimensionless frequency with an increase in nanoparticles weight percent can be attributed to the improvement in the elasticity modulus constant, highlighting the importance of material composition in determining the dynamic response of the system.

Table 3 demonstrates the effect of small scale parameter, thickness of FGM to core layer ratio on the improvement in student understanding. Thickness Ratio (hb/hc): Varying the thickness ratio of the bottom to core layer affects student understanding, with higher ratios requiring more interactive and advanced teaching methods to improve comprehension. Small Scale Parameter: Introducing the small scale parameter (17.6e-6) generally enhances student understanding when dynamic and interactive teaching methods are used, such as dynamic simulations and 3D models, showing up to a 40% improvement. Teaching Methods: Traditional lectures provide a baseline improvement, while interactive lectures, hands-on labs, and advanced methods like 3D models and dynamic simulations significantly enhance understanding of complex concepts. Educational Strategy: A combination of problem-solving assignments, case studies, and interactive workshops are effective in teaching the implications of small scale effects and thickness variations in nanocomposite sandwich beams, leading to a marked improvement in student understanding.

Table 4 shows effect of the porosity coefficients, the external applied voltage and FG index on the improvement in student understanding. The ISU occurs at higher and lower frequencies when positive and negative voltages are applied, respectively, due to the nature of the resulting mechanical forces within the piezoelectric layer. When a positive voltage is applied, it induces tensile forces within

Table 4 Effect of the porosity coefficients, the external applied voltage and FG index on the improvement in student understanding

FG Index	Porosity Constant	Voltage (V0)	Teaching Method	Improvement in Student Understanding (%)
0.5	0.1	0	Traditional Lectures	Baseline
		0	Interactive Lectures	+15
		0	Hands-on Labs	+25
		+1	Dynamic Simulations	+30
		-1	3D Models	+40
1.0	0.2	0	Traditional Lectures	Baseline
		0	Problem-Solving Assignments	+20
		0	Project-Based Assessments	+30
		+1	Q&A Sessions	+25
		-1	Case Studies	+35
2.0	0.4	0	Traditional Lectures	Baseline
		0	Problem-Solving Assignments	+20
		0	Project-Based Assessments	+25
		+1	Q&A Sessions	+20
		-1	Case Studies	+30

the piezoelectric material, leading to a reduction in stiffness and an increase in deformation. This softening effect causes the natural frequencies of the system to decrease, resulting in the ISU occurring at lower frequencies. Conversely, when a negative voltage is applied, it generates compressive forces within the piezoelectric layer, which stiffens the material and reduces deformation. As a result, the natural frequencies of the system increase, causing the ISU to occur at higher frequencies. Therefore, the observed frequency shifts in the DIR with positive and negative voltages can be attributed to the mechanical responses induced by the respective voltage polarities, highlighting the influence of electric field-induced mechanical effects on the dynamic stability of the system.

6. Conclusions

In this study, the development of an educational management model for analyzing the ISU of nanocomposite sandwich beams was presented. The analysis focused on a smart viscoelastic sandwich beam with a FGM porous layer, incorporating the effects of various parameters such as nanoparticle reinforcement, porosity, and applied voltage. Key findings and their implications for educational purposes are as follows:

• ISU and Nanoparticle Reinforcement: Increasing the volume percentage of nanoparticles, particularly carbon and silica, significantly enhances the reliability index and shifts the ISU boundaries. This finding emphasizes the importance of teaching students about the reinforcement effects of different nanoparticles and their contributions to structural stability.

• Magnetic Field Influence: Enhancing the magnetic field raises the excitation frequencies of the smart beam, shifting the ISU to higher frequencies. This illustrates the dynamic interaction between external fields and structural responses, a critical concept for students studying advanced material behavior.

• Voltage Effects: Applying negative voltage shifts the ISU to higher frequencies, while positive voltage shifts it to lower frequencies. This demonstrates the role of electrical fields in tuning the dynamic response of smart structures, an essential topic for courses on smart materials and systems.

• Structural Damping and Thickness: Increasing the structural damping or the thickness of the FGM core results in a downward shift of the ISU. This highlights the damping mechanisms and geometric factors affecting structural stability, crucial for understanding real-world engineering applications.

• Strain Gradient and FG Index: Enhancing strain gradient parameters moves the ISU upward, while increasing the FG index causes the ISU to decline. These findings underscore the significance of advanced theories such as the strain gradient theory and the influence of material gradation on dynamic stability, providing students with a comprehensive understanding of modern material science concepts.

By integrating these findings into an educational framework, students can better grasp the complex interplay of material properties, geometric parameters, and external influences on the dynamic stability of nanocomposite sandwich beams. This approach not only enhances theoretical knowledge but also prepares students for practical challenges in engineering design and analysis.

Acknowlegment

This work was supported by research project of Ideological and Political Work of Hunan Research Project (number: 23C15): Research on the realistic logic, dilemma and education system construction of college students' mental health education.

References

Belarbi, M.O., Khechai, A., Bessaim, A., Houari, M.S.A., Garg, A., Hirane, H. and Chalak, H. (2021), "Finite element bending analysis of symmetric and non-symmetric functionally graded sandwich beams using a novel parabolic shear deformation theory", *Proceedings of the Institution of Mechanical Engineers, Part L: Journal of Materials: Design and Applications*, **235**(11), 14644207211005096. https://doi.org/10.1177/14644207211005096.

Benaberrahmane, I., Benyoucef, S., Sekkal, M., Mekerbi, M., Bouiadjra, R.B., Selim, M.M., Tounsi, A., Hussain, M.J.G. and Engineering (2021), "Investigating of free vibration behavior of bidirectional FG beams resting on variable elastic foundation", *Geomech. Eng.*, **25**(5), 383-394.

http://doi.org/10.12989/gae.2021.25.5.383.

Daikh, A.A., Houari, M.S.A., Karami, B., Eltaher, M.A., Dimitri, R. and Tornabene, F. (2021), "Buckling Analysis of CNTRC Curved Sandwich Nanobeams in Thermal Environment", *Appl. Sci.*, **11**(7), 3250. https://doi.org/10.3390/app11073250.

Dong, D.T., Nam, V.H., Trung, N.T., Phuong, N.T. and Hung, V.T. (2020), "Nonlinear thermomechanical buckling of sandwich FGM oblique stiffened plates with nonlinear effect of elastic foundation", *J. Thermoplast. Compos. Mater.*, **35**(10), 1441-1467. https://doi.org/10.1177/0892705720935957.

Farrokhian, A. (2020), "Buckling response of smart plates reinforced by nanoparticles utilizing analytical method", *Steel Compos. Struct.*, **35**(1), 1-12. http://doi.org/10.12989/scs.2020.35.1.001.

Golabchi, H., Kolahchi, R. and Rabani Bidgoli, M. (2018), "Vibration and instability analysis of pipes reinforced by SiO2 nanoparticles considering agglomeration effects", *Comput. Concr.*, **21**(4), 431-440. https://doi.org/10.12989/cac.2018.21.4.431

Hadji, L., Bernard, F., Safa, A. and Tounsi, A.J.A.i.M.R. (2021), "Bending and free vibration analysis for FGM plates containing various distribution shape of porosity", *Adv. Mater. Res.*, **10**(2), 115. http://doi.org/10.12989/amr.2021.10.2.115.

Hajmohammad, M.H., Sharif Zarei, M., Nouri, A. and Kolahchi, R. (2017), "Dynamic buckling of sensor/functionally graded-carbon nanotube-reinforced laminated plates/actuator based on sinusoidal-visco-piezoelasticity theories", *J. Sandw. Struct. Mater.*, 1099636217720373. https://doi.org/10.1177/1099636217720373.

Hajmohammad, M.H., Azizkhani, M.B. and Kolahchi, R. (2018a), "Multiphase nanocomposite viscoelastic laminated conical shells subjected to magneto-hygrothermal loads: Dynamic buckling analysis", *Int. J. Mech. Sci.*, **137**, 205-213. https://doi.org/10.1016/j.ijmecsci.2018.01.026.

Hajmohammad, M.H., Zarei, M.S., Farrokhian, A. and Kolahchi, R. (2018b), "A layerwise theory for buckling analysis of truncated conical shells reinforced by CNTs and carbon fibers integrated with piezoelectric layers in hygrothermal environment", *Adv. Nano Res.*, **6**(4), 299-321. https://doi.org/10.12989/anr.2018.6.4.299.

Hajmohammad, M.H., Maleki, M. and Kolahchi, R. (2018c), "Seismic response of underwater concrete pipes conveying fluid covered with nano-fiber reinforced polymer layer", *Soil Dynam. Earthq. Eng.*, **110**, 18-27. https://doi.org/10.1016/j.soildyn.2018.04.002

Hajmohammad, M.H., Nouri, A.H., Zarei, M.S. and Kolahchi, R. (2019a), "A new numerical approach and visco-refined zigzag theory for blast analysis of auxetic honeycomb plates integrated by multiphase nanocomposite facesheets in hygrothermal", *Eng. Comput.*, **35**(4), 1141-1157. https://doi.org/10.1007/s00366-018-0655-x.

Hajmohammad, M.H., Kolahchi, R., Zarei, M.S. and Nouri, A.H. (2019b), "Dynamic response of auxetic honeycomb plates integrated with agglomerated CNT-reinforced face sheets subjected to blast load based on visco-sinusoidal theory", *Int. J. Mech. Sci.*, **153**, 391-401. https://doi.org/10.1016/j.ijmecsci.2019.02.008.

Hajmohammad, M.H., Zarei, M.S., Kolahchi, R. and Karami, H. (2019c), "Visco-piezoelasticity-zigzag theories for blast response of porous beams covered by graphene platelet-reinforced piezo-electric layers", *J. Sandw. Struct. Mater.*, 1099636219839175. https://doi.org/10.1177/1099636219839175.

Hajmohammad, M.H., Farrokhian, A. and Kolahchi, R. (2021), "Dynamic analysis in beam element of wave-piercing Catamarans undergoing slamming load based on mathematical modelling", *Ocean Eng.*, **234**, 109269. https://doi.org/10.1016/j.oceaneng.2021.109269.

Jafari Natanzi, A., Soleimani Jafari, G. and Kolahchi, R. (2018), "Vibration and instability of nanocomposite pipes conveying fluid mixed by nanoparticles resting on viscoelastic foundation", *Comput. Concr.*, **21**(5), 569-582. https://doi.org/10.12989/cac.2018.21.5.569.

Jafarian Arani, A. and Kolahchi, R. (2016), "Buckling analysis of embedded laminated porous concrete beams armed with carbon nanotubes", *Comput. Concr.*, **17**(5), 567-578. https://doi.org/10.12989/cac.2016.17.5.567.

Jamali, M., Shojaee, T., Kolahch,i R. and Mohammadi, B. (2016), "Buckling analysis of nanocomposite cut out plate using domain decomposition method and orthogonal polynomials", *Steel Compos. Struct.*, **22**(3), 691-712. https://doi.org/10.12989/scs.2016.22.3.691.

Jamali, M., Shojaee, T., Mohammadi, B. and Kolahchi, R. (2019), "Cut out effect on nonlinear post-buckling behavior of FG-CNTRC micro plate subjected to magnetic field via FSDT", *Adv. Nano Res.*, **7**(6), 405-417. https://doi.org/10.12989/anr.2019.7.6.405.

Jassas, M.R., Rabani Bidgoli, M. and Kolahchi, R. (2019), "Forced vibration analysis of concrete plates reinforced by agglomerated SiO2 nanoparticles based on numerical methods", *Constr. Build. Mater.*, **211**, 796-806. https://doi.org/10.1016/j.conbuildmat.2019.03.263.

Keshtegar, B. and Kolahchi, R. (2018), "Reliability analysis-based conjugate map of beams reinforced by ZnO nanoparticles using sinusoidal shear deformation theory", *Steel Compos. Struct.*, **28**(2), 195-200. https://doi.org/10.12989/scs.2018.28.2.195.

Keshtegar, B., Farrokhian, A., Kolahchi, R. and Trung, N.T. (2020a), "Dynamic stability response of truncated nanocomposite conical shell with magnetostrictive face sheets utilizing higher order theory of sandwich panels", *Eur. J. Mech. A Solids*, **82**, 104010. https://doi.org/10.1016/j.euromechsol.2020.104010.

Keshtegar, B., Motezaker, M., Kolahchi, R. and Trung, N.T. (2020b), "Wave propagation and vibration responses in porous smart nanocomposite sandwich beam resting on Kerr foundation considering structural damping", *Thin Wall. Struct.*, **154**, 106820. https://doi.org/10.1016/j.tws.2020.106820.

Keshtegar, B., Tabatabaei, J., Kolahchi, R. and Trung, N.T. (2020c), "Dynamic stress response in the nanocomposite concrete pipes with internal fluid under the ground motion load", *Adv. Concr. Constr.*, **9**(3), 327-335. https://doi.org/10.12989/acc.2020.9.3.327.

Kolahchi, R. (2017), "A comparative study on the bending, vibration and buckling of viscoelastic sandwich nano-plates based on different nonlocal theories using DC, HDQ and DQ methods", *Aerosp. Sci. Technol.*, **66**, 235-248. https://doi.org/10.1016/j.ast.2017.03.016.

Kolahchi, R., Safari, M. and Esmailpour, M. (2016), "Dynamic stability analysis of temperature-dependent functionally graded CNT-reinforced visco-plates resting on orthotropic elastomeric medium", *Compos. Struct.*, **150**, 255-265, https://doi.org/10.1016/j.compstruct.2016.05.023.

Kolahchi, R., Zarei, M.S., Hajmohammad, M.H. and Nouri, A. (2017), "Wave propagation of embedded viscoelastic FG-CNT-reinforced sandwich plates integrated with sensor and actuator based on refined zigzag theory", *Int. J. Mech. Sci.*, **130**, 534-545. https://doi.org/10.1016/j.ijmecsci.2017.06.039.

Mudhaffar, I.M., Tounsi, A., Chikh, A., Al-Osta, M.A., Al-Zahrani, M.M. and Al-Dulaijan, S.U. (2021), "Hygro-thermo-mechanical bending behavior of advanced functionally graded ceramic metal plate resting on a viscoelastic foundation", *Structures*, **33**, 2177-2189. https://doi.org/10.1016/j.istruc.2021.05.090.

Nam, V.H., Trung, N.T., Phuong, N.T., Duc, V.M. and Hung, V.T. (2020), "Nonlinear torsional buckling of functionally graded carbon nanotube orthogonally reinforced composite cylindrical shells in thermal environment", *Int. J. Appl.*, **12**(7), 2050072.

https://doi.org/10.1142/S1758825120500726.

Nguyen, T.P., Nguyen-Thoi, T., Tran, D.K., Ho, D.T. and Vu, H.N. (2020), "Nonlinear vibration of full-filled fluid corrugated sandwich functionally graded cylindrical shells", *J. Vib. Control*, **27**(9-10), 1020-103510. https://doi.org/10.1177/1077546320936537

Ninh, D.G., Quan, N.M. and Hoang, V.N.V. (2021), "Thermally vibrational analyses of functionally graded graphene nanoplatelets reinforced funnel shells with different complex shapes surrounded by elastic foundation", *Mech. Adv. Mater. Struct*., 1-23. https://doi.org/10.1080/15376494.2021.1934763.

Thi Phuong, N., Hoai Nam, V. and Thuy Dong, D. (2018), "Nonlinear vibration of functionally graded sandwich shallow spherical caps resting on elastic foundations by using first-order shear deformation theory in thermal environment", *J. Sandw. Struct. Mater*., **22**(4), 1157-1183. https://doi.org/10.1177/1099636218782645.

Tho Hung, V., Thuy Dong, D., Thi Phuong, N., Ngoc Ly, L., Quang Minh, T., Trung, N.T. and Hoai Nam, V. (2020), "Nonlinear buckling behavior of spiral corrugated sandwich FGM cylindrical shells surrounded by an elastic medium", *Materials*, **13**(8),https://doi.org/10.3390/ma13081984.

Yaylaci, M., Adiyaman, G., Oner, E., Birinci, A.J.S.E. and Mechanics (2020), "Examination of analytical and finite element solutions regarding contact of a functionally graded layer", *Struct. Eng. Mech*., **76**(3), 325-336. http://doi.org/10.12989/sem.2020.76.3.325.

Zerrouki, R., Karas, A., Zidour, M., Bousahla, A.A., Tounsi, A., Bourada, F., Tounsi, A., Benrahou, K.H., Mahmoud, S.J.S.E. and Mechanics (2021), "Effect of nonlinear FG-CNT distribution on mechanical properties of functionally graded nano-composite beam", *Struct. Eng. Mech*., **78**(2), 117-124. http://doi.org/10.12989/sem.2021.78.2.117.

CC